WIND ENERGY
Wind Energ. 2012; **15**:289–303
Published online 4 April 2011 in Wiley Online Library (wileyonlinelibrary.com). DOI: 10.1002/we.468

RESEARCH ARTICLE

A method for defining wind turbine setback standards

Jonathan Rogers[1], Nathan Slegers[2] and Mark Costello[1]

[1] School of Aerospace Engineering, Georgia Institute of Technology, Atlanta, Georgia 30332, USA
[2] School of Mechanical and Aerospace Engineering, University of Alabama in Huntsville, Huntsville, Alabama 35899, USA

ABSTRACT

Setback distances established by regulatory authorities to minimize the probability of blade fragment impact with roads, structures and infrastructure can often have a significant impact on wind farm development. However, these minimum distance requirements typically rely on arbitrary rules of thumb and are not based on a physical or probabilistic analysis of blade throw. The work reported here uses a probabilistic approach to evaluate the effectiveness of current standards and to propose a new technique for determining setback distances. This is accomplished through the use of a dynamic model of wind turbine blade failure coupled with Monte Carlo simulation techniques applied to three different wind turbines. It is first shown that common setback standards based on turbine height and blade radius provide inconsistent and inadequate protection against blade throw. Then, using a simplified dynamic analysis of a thrown blade fragment, it is shown that the release velocity of the blade fragment is the critical factor in determining the maximum distance fragments are likely to travel. The importance of release velocity is further verified through simulation results. Finally, a new method for developing setback standards is proposed based on an acceptable level of risk. Given specific wind turbine operational parameters and a set of failure probabilities, the new method leverages realistic blade throw modeling to produce setback standards with a valid physical foundation.

Correspondence
Jonathan Rogers, School of Aerospace Engineering, Georgia Institute of Technology, 270 Ferst Drive, Atlanta, Georgia 30332, USA.
E-mail: jrogers8@gmail.com

Received 1 November 2010; Revised 14 February 2011; Accepted 15 February 2011

NOMENCLATURE

h	height of turbine rotor hub
$\boldsymbol{I}$	blade fragment moment of inertia matrix about mass center expressed in blade-fixed frame
$\vec{\boldsymbol{I}}_{\mathrm{B}}, \vec{\boldsymbol{J}}_{\mathrm{B}}, \vec{\boldsymbol{K}}_{\mathrm{B}}$	unit vectors in frame B
L, M, N	total external moment exerted on blade fragment about mass center expressed in blade-fixed frame
l	distance from rotor hub to nacelle vertical axis of rotation
m	mass of blade fragment
q_0, q_1, q_2, q_3	quaternion orientation parameters of the blade fragment
p, q, r	angular velocity components of the blade fragment expressed in the blade-fixed reference frame
R	rotor radius
r_{CG}	distance from blade root to blade
$\boldsymbol{T}_{\mathrm{IB}}$	transformation matrix from blade-fixed reference frame to inertial reference frame
u, v, w	translational velocity components of the blade fragment mass center expressed in the blade-fixed frame
x, y, z	position coordinates of the blade fragment mass center expressed in the inertial frame
X, Y, Z	total external force exerted on blade fragment
θ	rotor plane cant angle
ψ	rotor plane azimuthal angle
φ	rotor blade roll angle
Ω	rotor rotational speed

1. INTRODUCTION

Increasing demand for wind energy production has led to unprecedented wind farm development over the past decade. State and local regulations specifying required setback distances between wind turbines and property lines, roads and other infrastructure can have a significant impact on the number of turbines that can be installed on a given site. These setback standards are intended to protect people and property from rotor blade fragments released from failed wind turbine blades. However, required setbacks are often based on rules of thumb involving some combination of turbine height and blade radius and typically have little or no rigorous physical foundation. There is currently a strong demand for re-evaluation of turbine setback distances in view of both increased turbine reliability and the desire to install more large turbines on small parcels of land. Specifically, it would be desirable to provide a technique that allows regulators and wind farm developers to determine setback requirements given a specific turbine model, the site parameters and an acceptable level of risk. This new methodology would provide developers, regulators and insurers with a setback corresponding to a specific risk level that is generated through probabilistic dynamic modeling techniques rather than arbitrary rules of thumb.

Several investigators have studied blade fragment release from a failed wind turbine blade, beginning with Eggwertz *et al.*[1] The authors used a point-mass dynamic model to show that the probability of blade impact with the ground beyond 1.8 times the overall turbine height was low. Similarly, Macqueen *et al.*[2] demonstrated through the use of a point-mass model that a person being struck by a blade fragment at a distance greater than 220 m from the turbine base was extremely unlikely. Turner,[3] also employing a point-mass model, used Monte Carlo simulation techniques to construct a statistical distribution of blade fragment impact. Eggers *et al.*[4] likewise exercised a point-mass model for blade fragments using Monte Carlo methods and obtained results similar to that of Macqueen *et al.*[2] The first investigation of fragment throw using full six-degree-of-freedom modeling was performed by Montgomerie,[5] who reported very high maximum distances. Sørensen[6,7] also analysed full rigid body motion of the blade fragment and reported how maximum throw distance varied as a function of aerodynamic characteristics, fragment center of gravity location, pitch angle and wind velocity. Turner[8] provided a similar rigid body analysis and obtained results similar to those of Sørensen.[6,7] Finally, Slegers *et al.*[9] investigated blade fragment impact with power transmission lines. It was shown that transmission line impact probability is a strong function of line distance from the turbine as well as orientation of the line with respect to the axis of rotor rotation. Whereas numerous researchers have simulated the blade throw problem to determine expected impact distances, Rademakers and Braam[10] have conducted a statistical analysis of reported blade failures to determine the overall probability of blade failure occurring. Their analysis suggests an overall probability of blade failure of 2.6×10^{-4} per turbine per year, or approximately 1 in 3800. This is a non-trivial probability that further highlights the need for universal and effective setback standards to protect against blade throws.

Despite significant research analysing the physics of blade fragment release and failure probabilities, many previous investigations lack clear guidance in determining safe setback distances. Furthermore, the variety of models and assumptions made by each investigator has led to differing technical conclusions. The result is that technical analyses of blade throw are often ignored and rules of thumb are employed at a local level. In California, for instance, five different counties use a variety of setback standards all based on overall turbine height to ensure the safety of the surrounding buildings, properties and roads.[11]

The work reported here first demonstrates that many setback standards currently in use provide little or no protection against blade fragment throw for several example turbine designs. A six-degree-of-freedom model is used to simulate a failed rotor blade fragment in free flight and is exercised through Monte Carlo simulations to obtain a statistical distribution of blade fragment impact with the ground. It is shown that for all three turbines studied, a significant portion of blade fragments impact outside the distance specified by example setback standards that are currently in use. Then, by using a simplified dynamic model of blade fragment motion, it is shown analytically that blade release velocity plays the largest role in maximum throw distance. This is verified through Monte Carlo simulation results. Finally, a new methodology is proposed to determine setback standards based on turbine physical parameters, failure probabilities and the regulator's acceptable level of risk. This methodology allows the setback developer to mitigate risk using probabilistic dynamic modeling of blade failure, thereby avoiding the use of arbitrary rules of thumb.

2. DYNAMIC MODEL AND SIMULATION METHODOLOGY

2.1. Blade throw dynamic model

An abbreviated version of the dynamic model used to simulate the flight of a released blade fragment is presented here. A full description of the dynamic model can be found in Slegers *et al.*[9] As shown in Figures 1 and 2, three reference frames are employed in the dynamic model of blade motion, namely, the ground-based frame I, the turbine-fixed frame R and the blade-fixed frame B. The blade-fixed reference frame B is oriented such that the $\vec{\boldsymbol{K}}_{\mathrm{B}}$ axis is aligned with the blade spanwise axis. The inertial reference frame is oriented such that $\vec{\boldsymbol{K}}_{\mathrm{I}}$ points straight down and $\vec{\boldsymbol{I}}_{\mathrm{I}}$ lies in a plane formed by

Wind Energ. 2012; **15**:289–303 © 2011 John Wiley & Sons, Ltd.
DOI: 10.1002/we

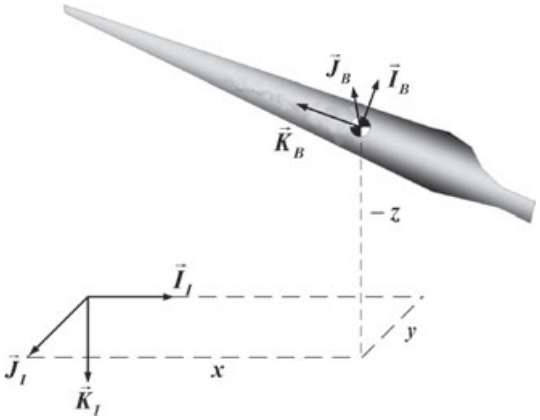

Figure 1. Blade reference frame schematic.

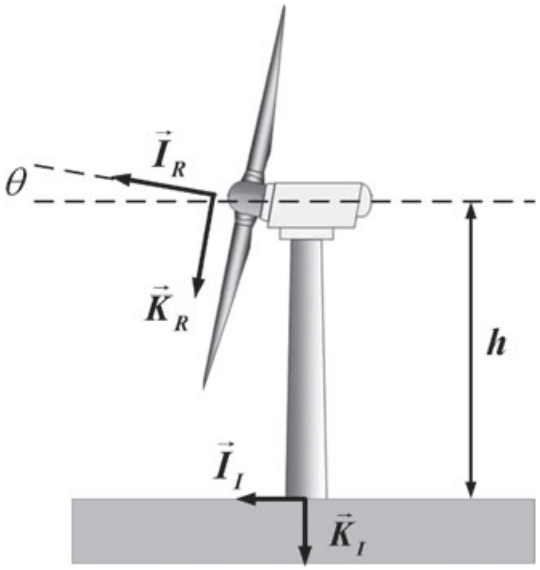

Figure 2. Turbine reference frame schematic.

the rotor hub and the turbine nacelle. The R frame is fixed to the turbine, with $\vec{I}_{\mathrm{R}}$ aligned with the rotor's axis of rotation. Figures 2–4 demonstrate blade geometry including turbine azimuth angle ψ_{T}, wind azimuth angle ψ_{W}, hub cant angle θ and blade roll angle φ. As shown in Figure 4, blade roll angle is referenced from the $\vec{K}_{\mathrm{R}}$ axis. Note that within this section, the following shorthand notation with be used for trigonometric functions: $\sin(\alpha) = \boldsymbol{s}_\alpha$, $\cos(\alpha) = \boldsymbol{c}_\alpha$ and $\tan(\alpha) = \boldsymbol{t}_\alpha$.

The dynamic model of the blade fragment in free flight consists of 13 scalar differential equations, given by equations (1)–(4). The states of the system are defined as follows: blade mass center position with respect to the inertial frame (x, y, z), mass center translational velocity resolved in the blade-fixed frame (u, v, w), quaternion rotational parameters describing blade orientation (q_0, q_1, q_2, q_3) and angular velocity components resolved in the blade-fixed frame (p, q, r).

$$\begin{Bmatrix} \dot{\boldsymbol{x}} \\ \dot{\boldsymbol{y}} \\ \dot{\boldsymbol{z}} \end{Bmatrix} = [\boldsymbol{T}_{\mathrm{IB}}] \begin{Bmatrix} u \\ v \\ w \end{Bmatrix} \tag{1}$$

$$\begin{Bmatrix} \dot{\boldsymbol{q}}_0 \\ \dot{\boldsymbol{q}}_1 \\ \dot{\boldsymbol{q}}_2 \\ \dot{\boldsymbol{q}}_3 \end{Bmatrix} = \frac{1}{2} \begin{bmatrix} 0 & -p & -q & -r \\ p & 0 & r & -q \\ q & -r & 0 & p \\ r & q & -p & 0 \end{bmatrix} \begin{Bmatrix} q_0 \\ q_1 \\ q_2 \\ q_3 \end{Bmatrix} \tag{2}$$

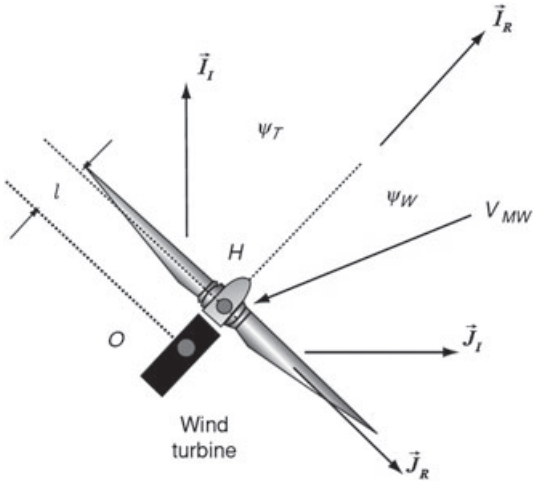

Figure 3. Rotor angle definitions.

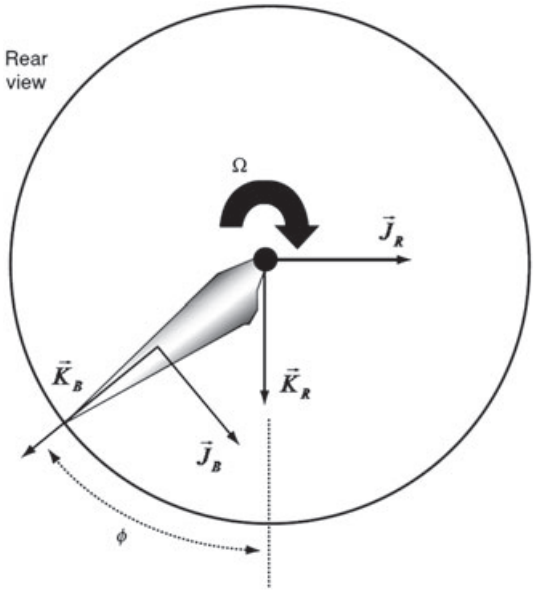

Figure 4. Blade roll angle definition.

$$\begin{Bmatrix} \dot{u} \\ \dot{v} \\ \dot{w} \end{Bmatrix} = \begin{Bmatrix} X/m \\ Y/m \\ Z/m \end{Bmatrix} - \begin{bmatrix} 0 & -r & q \\ r & 0 & -p \\ -q & p & 0 \end{bmatrix} \begin{Bmatrix} u \\ v \\ w \end{Bmatrix} \tag{3}$$

$$\begin{Bmatrix} \dot{p} \\ \dot{q} \\ \dot{r} \end{Bmatrix} = [I]^{-1} \left(\begin{Bmatrix} L \\ M \\ N \end{Bmatrix} - \begin{bmatrix} 0 & -r & q \\ r & 0 & -p \\ -q & p & 0 \end{bmatrix} [I] \begin{Bmatrix} p \\ q \\ r \end{Bmatrix} \right) \tag{4}$$

Note that in equations (3) and (4), the terms X, Y, Z and L, M, N, respectively, denote the total external force and the moment exerted on the blade in the blade-fixed frame. External force on the blade consists of the sum of aerodynamic and gravity forces, whereas aerodynamic moment is the sole source of moments on the blade. The matrix $\boldsymbol{T}_{\mathrm{IB}}$ is the transformation matrix from the blade-fixed to inertial frames, and the matrix $\boldsymbol{I}$ is the moment of inertia matrix of the blade about its mass center with respect to blade-fixed coordinates. Aerodynamic forces were calculated using strip theory by considering the blade as a lifting surface with a general angle of attack. This angle of attack is calculated within the simulation given

Wind Energ. 2012; **15**:289–303 © 2011 John Wiley & Sons, Ltd.
DOI: 10.1002/we

blade orientation and velocity and subsequently used to generate aerodynamic forces and moments on the blade. Details of aerodynamic forces, moments as well as the weight force are omitted here for brevity; however, a full description is provided in Slegers.[9]

Given a set of blade fragment release conditions, equations (1)–(4) can be integrated numerically forward in time using a Runge–Kutta algorithm until blade fragment mass center impacted with the ground. The simulation architecture, written in FORTRAN, was optimized to run Monte Carlo cases efficiently. Simulation cases were ran in an automated fashion on a computing cluster, allowing thousands of blade throws to be simulated in a reasonable amount of time.

2.2. Monte Carlo simulation description

The dynamic simulation described previously is used to generate a probabilistic analysis of wind turbine setback standards. This is accomplished through the use of tens of thousands of simulations with randomized initial conditions. The Monte Carlo simulation architecture generates initial conditions for each fragment throw by varying six different release parameters in a random fashion. These six parameters are blade roll angle (φ), cant angle (θ), azimuthal angle (ψ), rotor rotational speed (Ω), wind speed and wind angle (ψ_W). Note that all Monte Carlo results are relative to a nominal prevailing wind value, with the assumption that the turbine is nominally facing into the wind. All parameter distributions are assumed to be normal with the exception of roll angle and wind speed. Blade roll angle at release is a uniform random variable between 0 and 360°. Wind speed is varied according to a Rayleigh distribution assuming a median value of 8.5 m s^{-1}. Note that this distribution reflects standard winds expected at an International Electrotechnical Commission Class 2 wind farm installation. Table I describes the statistics associated with each parameter for all cases in Section 3.

Given a randomized set of these six parameters, as well as physical characteristics of the turbine, the initial conditions for all the states of the blade fragment at release were generated. Blade fragment position and velocity at the time of release were determined using

$$\begin{Bmatrix} x \\ y \\ z \end{Bmatrix} = \begin{Bmatrix} lc_{\psi_T} \\ ls_{\psi_T} \\ -h \end{Bmatrix} + [\boldsymbol{T}_{IB}] \begin{Bmatrix} 0 \\ 0 \\ r_{CG} \end{Bmatrix} \tag{5}$$

$$\begin{Bmatrix} u \\ v \\ w \end{Bmatrix} = \begin{Bmatrix} 0 \\ -r_{CG}\Omega \\ 0 \end{Bmatrix} \tag{6}$$

where r_{CG} represents the distance from the blade root to the blade center of mass and l is the distance between the rotor hub and the origin. The initial orientation and the angular velocity of the thrown blade fragments were calculated according to

$$q_0 = \cos\left(\frac{\psi_T}{2}\right)\cos\left(\frac{\theta}{2}\right)\cos\left(\frac{\phi}{2}\right) + \sin\left(\frac{\psi_T}{2}\right)\sin\left(\frac{\theta}{2}\right)\sin\left(\frac{\phi}{2}\right) \tag{7}$$

$$q_1 = \cos\left(\frac{\psi_T}{2}\right)\cos\left(\frac{\theta}{2}\right)\cos\left(\frac{\phi}{2}\right) - \sin\left(\frac{\psi_T}{2}\right)\sin\left(\frac{\theta}{2}\right)\cos\left(\frac{\phi}{2}\right) \tag{8}$$

$$q_2 = \cos\left(\frac{\psi_T}{2}\right)\sin\left(\frac{\theta}{2}\right)\cos\left(\frac{\phi}{2}\right) + \sin\left(\frac{\psi_T}{2}\right)\cos\left(\frac{\theta}{2}\right)\sin\left(\frac{\phi}{2}\right) \tag{9}$$

$$q_3 = \sin\left(\frac{\psi_T}{2}\right)\cos\left(\frac{\theta}{2}\right)\cos\left(\frac{\phi}{2}\right) - \cos\left(\frac{\psi_T}{2}\right)\sin\left(\frac{\theta}{2}\right)\sin\left(\frac{\phi}{2}\right) \tag{10}$$

Table I. Monte Carlo simulation random parameter statistics.

Parameter	Mean	Standard deviation
Roll angle, φ (degree)	0.0	−180 to 180 (uniform)
Cant angle, θ (degree)	4.0	1.0
Azimuthal angle, ψ_T (degree)	0.0	10.0
Rotor rotational speed (rad s^{-1})	Turbine dependent	0.1
Wind speed (m s^{-1})	Rayleigh distribution, median 8.5 m s^{-1}	N/A
Wind angle ψ_W (degree)	0	3.0

$$\begin{Bmatrix} p \\ q \\ r \end{Bmatrix} = \begin{Bmatrix} \Omega \\ 0 \\ 0 \end{Bmatrix} \tag{11}$$

In Section 3, Monte Carlo simulations are performed for specific turbines using various blade fragment sizes. Because of a lack of statistics regarding the likely size of thrown blade fragments, all fragment sizes were considered. Thus, blade fragment size was varied using outer 20, 40, 60 and 80% and the entire blade throws.

2.3. Simplified point-mass blade fragment analysis

Although a ballistic point-mass analysis, especially one that neglects aerodynamic effects, is highly unsuitable for a detailed dynamic analysis of blade throw, it does provide simplified expressions that can assist in characterizing the most important factors in maximum lateral throw distance (longitudinal throw distance is largely a function of prevailing wind speed and thus cannot be addressed using an analysis that neglects aerodynamics). Because lateral throw distance is often the driving factor in setback development, this simplified analysis can provide rough bounds on expected setbacks for a given set of turbine parameters. Consider the scenario shown in Figure 5 in which a blade fragment at the tip of the blade is thrown at a certain height h_T and velocity v_T. We consider the blade fragment to be a point mass that impacts the ground at a lateral distance D from the turbine base after a time of flight T. Neglecting aerodynamics and considering only two dimensions, two equations of motion are given by

$$h - Rc_{\theta_T} + v_T s_{\theta_T} T - \frac{1}{2} g T^2 = 0 \tag{12}$$

$$D = v_T c_{\theta_T} T \tag{13}$$

where g denotes acceleration because of gravity. Eliminating T, equations (12) and (13) can be combined to yield

$$\frac{gD^2}{v_T^2} = 2\left(h - Rc_{\theta_T}\right) c_{\theta_T}^2 + 2Ds_{\theta_T} c_{\theta_T} \tag{14}$$

Equation (14) is a quadratic function of D. In order to find the angle of maximum throw as a function of h, R and v, one would typically take the derivative of equation (14) with respect to θ_T, set it equal to zero and solve for $\theta_{T_{\mathrm{MAX}}}$ as a function of h, R and v. However, a solution in closed form cannot be found since it is not possible to solve the resulting

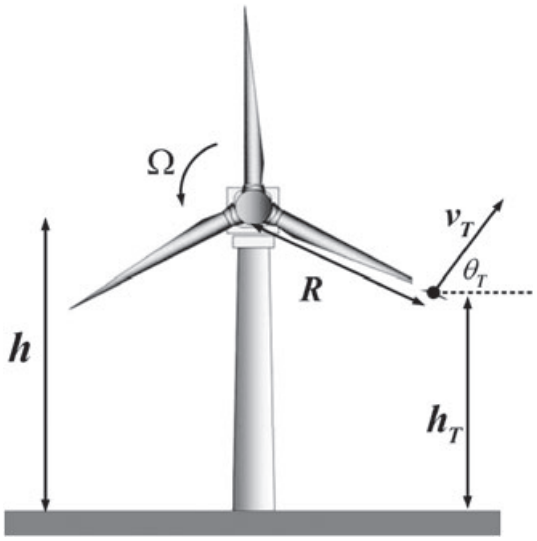

Figure 5. Blade fragment throw diagram.

Wind Energ. 2012; **15**:289–303 © 2011 John Wiley & Sons, Ltd.
DOI: 10.1002/we

expression for θ_T. Therefore, determination of the optimum release angle must be found numerically on a turbine-specific basis. Nevertheless, the roots of equation (14) are given by

$$D = \frac{v_T^2 s_{\theta_T} c_{\theta_T} \pm v_T^2 \sqrt{s_{\theta_T}^2 c_{\theta_T}^2 + 2\frac{g}{v_T^2}\left(h - Rc_{\theta_T}\right) c_{\theta_T}^2}}{g} \tag{15}$$

In equation (15), it is clear that the range of blade fragment flight is highly dependent on release velocity and release angle and less dependent on turbine height and blade radius. Specifically, lateral distance is a function of the square of the release velocity but only of the square root of turbine height and radius. Although in modern turbines there is some correlation between height, radius and release velocity (since blade fragments at the end of a longer blade travel faster than the fragments at the end of a shorter blade and longer blades are typically found on taller turbines), it is important to note that blade fragment velocity is the real driver behind maximum throw distance. As a result, setback standards based on mass center velocity of the minimum size fragment of concern will yield far more effective protection than a setback distance based on radius or height.

3. RESULTS

3.1. Monte Carlo simulation ground impact results

Monte Carlo simulations were performed for three example turbines of varying sizes, namely, 0.66, 1.5 and 3.0 MW. These turbines cover a range of size and power representative of those installed in typical modern wind farms. Table II lists the physical and operational parameters associated with each turbine.

Five Monte Carlo simulations consisting of 10,000 blade throws each were performed for each turbine, corresponding to the five blade fragment sizes of 20, 40, 60, 80 and 100% as previously outlined. As demonstrated in the Monte Carlo simulation results shown in Slegers,[9] smaller blade fragments consistently fly farther than larger fragments because of higher initial release velocity. Figures 6–11 show ground impact results of each Monte Carlo simulation for the three turbines for the 40% blade throw case. Figures 6, 8 and 10 show specific ground impact points for each turbine, whereas Figures 7, 9 and 11 show histograms of cross-range impact point location. Note that in Figures 6, 8 and 10, the turbine base is located at the origin. Also, note that the wind arrows in Figures 6, 8 and 10 specify the approximate direction of oncoming wind, since the exact direction is randomly distributed for each blade throw case. Although not shown here, plots of ground impacts for larger blade fragments showed a similar dispersion pattern but a smaller range of distances. In addition, histograms for all fragment sizes showed peaks directly below the turbine and slightly behind the turbine, as well as two lateral peaks near the maximum range of blade fragment throw. The peak directly below the turbine represents failures occurring at blade roll angles between approximately 235 and 325°, since these trajectories fly roughly straight down and are unaffected by winds because of the short time of flight. The more scattered distribution behind the turbine is due to fragments released straight upward (approximately between roll angles of 45 and 135°). The relatively long times of flight exhibited by these cases mean that they are more affected by winds.

Table II. Wind turbine physical and operational parameters.

Parameter	660 KW turbine	1.5 MW turbine	3.0 MW turbine
Blade radius (m)	23.5	35.0	45.0
Blade weight (N)	21,287	49,050	64,746
Blade CG from root (m)	11.75	17.5	22.5
Blade I_{XX} (kg m^2)	100,121	511,000	1,115,840
Blade I_{YY} (kg m^2)	99,891	510,000	1,113,830
Blade I_{ZZ} (kg m^2)	282	1233	2175
Rotational speed (rad s^{-1})	2.98	2.3	1.69
Maximum blade chord (m)	2.0	2.1	3.51
Tip blade chord (m)	0.34	0.94	0.45
Root blade pitch (degree)	10.5	10.5	16.6
Tip blade pitch (degree)	−0.5	−0.5	−0.85
Hub height (m)	50.0	80.0	80.0

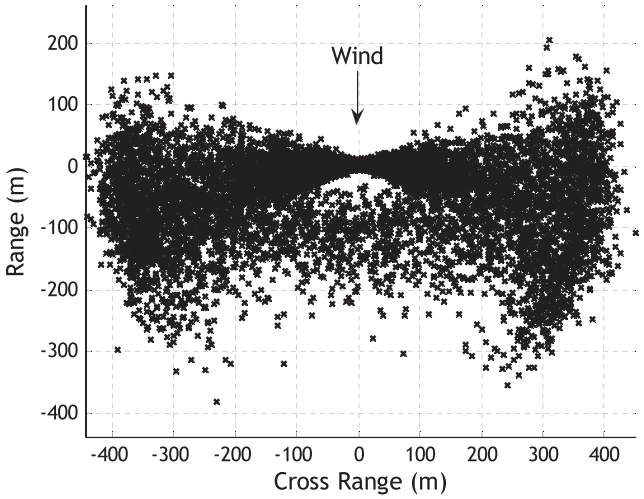

Figure 6. Ground impacts, 0.66 MW turbine, 40% fragment.

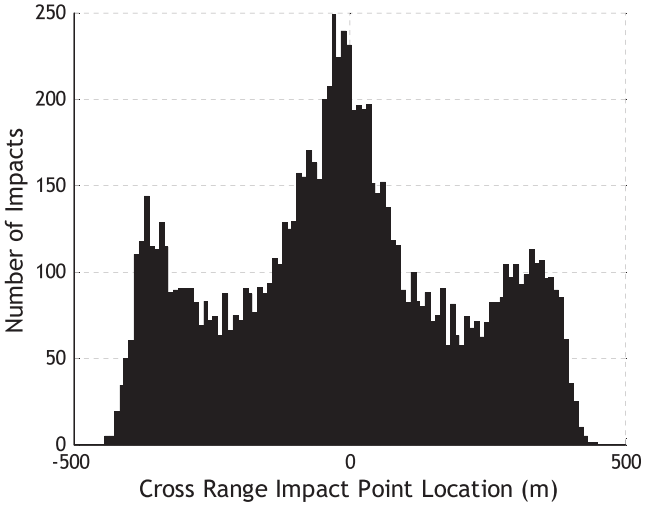

Figure 7. Histogram of cross-range impact location, 0.66 MW turbine, 40% fragment.

3.2. Evaluation of current setback standards

Current setback standards often rely on multiples of tower height, blade radius or both to form the basis for setback distances. To demonstrate the shortcomings typical of standards that rely on these parameters, two example setback distances are evaluated against the Monte Carlo data for three turbines shown in Section 3.1. The first setback originates from the minimum setback distances from the power transmission lines of Southern California Edison (SCE). SCE's Wholesale Generation Interconnection Technical Requirement document[12] states that 'the Producer shall not locate any part of a wind-driven wholesale generating unit … within three rotor blade diameters of an existing electric utility 220 or 500 kV transmission line right of way or future electric utility 220 or 500 kV transmission line right of way for which SCE may seek regulatory approval of construction.' The second example setback is taken from a report[13] prepared by the State of New York to provide guidance to local communities developing local ordinances governing wind energy. The report proposes the following setback requirement: 'The minimum setback distance between each wind turbine tower and all the surrounding property lines, overhead utility or transmission lines, other wind turbine towers, electrical substations, meteorological towers, public roads and dwellings shall be equal to no less than 1.5 times the sum of proposed structure height plus the rotor radius.' These two setbacks, given by three times the rotor diameter and one and a half times the total turbine height, are representative of many current setback standards and will be evaluated against the three example turbines described earlier.

Wind Energ. 2012; **15**:289–303 © 2011 John Wiley & Sons, Ltd.
DOI: 10.1002/we

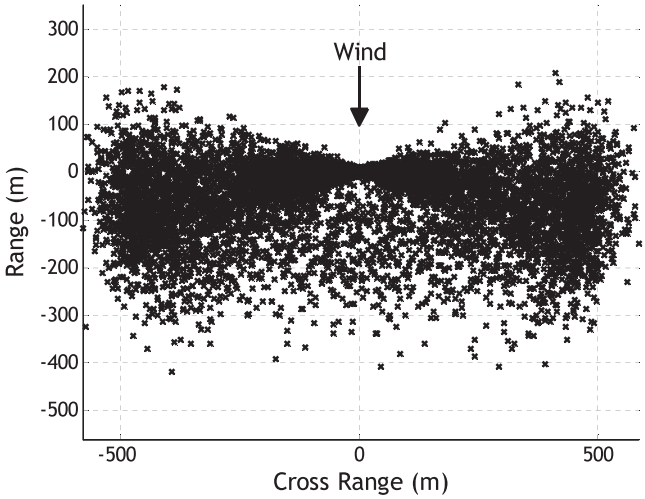

Figure 8. Ground impacts, 1.5 MW turbine, 40% fragment.

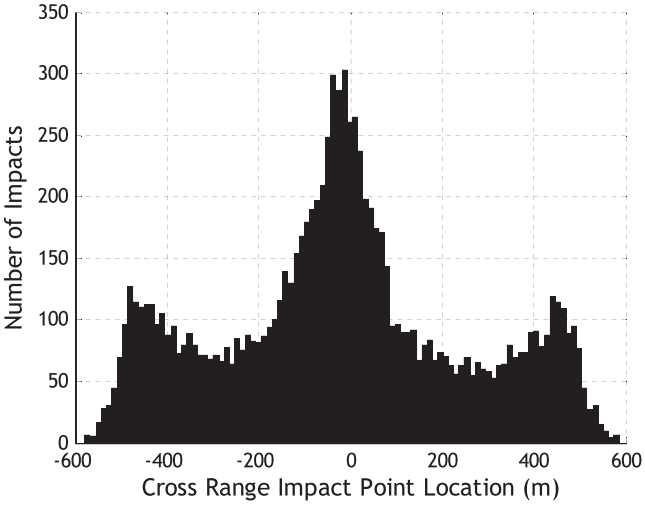

Figure 9. Histogram of cross-range impact location, 1.5 MW turbine, 40% fragment.

In order to evaluate the effectiveness of these example setbacks, circles of varying radius, centered at the turbine base, were considered for each turbine. For each circle, the percentage of blade fragment impacts that landed within this circle was determined. This was repeated for each blade fragment size, and the entire process was performed for each of the three turbines considered. Figures 12–14 show the percentage of impacts within circles of varying radii for each turbine. Also shown are the two example setback standards applied to the specific turbine under consideration.

Several interesting features are apparent in Figures 12–14. First, note that the percentage of impacts that fall within a circle varies somewhat linearly as the radius of the circle grows until greater than 95% of impacts are considered, especially for larger fragments. For smaller fragments at large throw distances, winds tend to have a more significant effect and carry the fragments farther because of longer times of flight, causing the non-linear behavior observed for small fragments at large throw distances. Second, as expected, smaller blade fragments fly farther, and thus, larger circles must be used to contain a given percentage of their impacts. Finally, note that neither of the example setbacks provides protection against a large percentage of blade fragment ground impacts for any of the three turbines. For the 0.66 MW turbine, 60–65% of ground impacts for fragment sizes of 20% fall outside these example setbacks. For the 1.5 and 3.0 MW turbines, 40–50% of ground impacts for 20% blade fragments fall outside these example setbacks. It is important to note that 20% blade fragments are close to 10 m long and can pose a significant hazard.

This analysis of representative setback standards leads to the conclusion that current methods for determining proper setback standards are inadequate. In the cases considered here, setback distances provide little or no reasonable protection

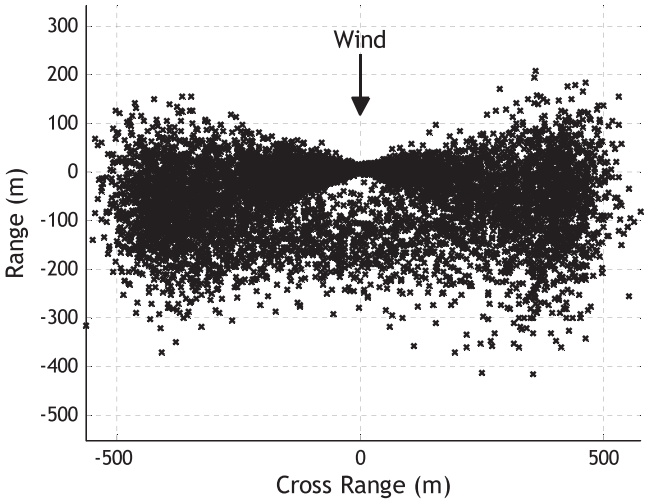

Figure 10. Ground impacts, 3.0 MW turbine, 40% fragment.

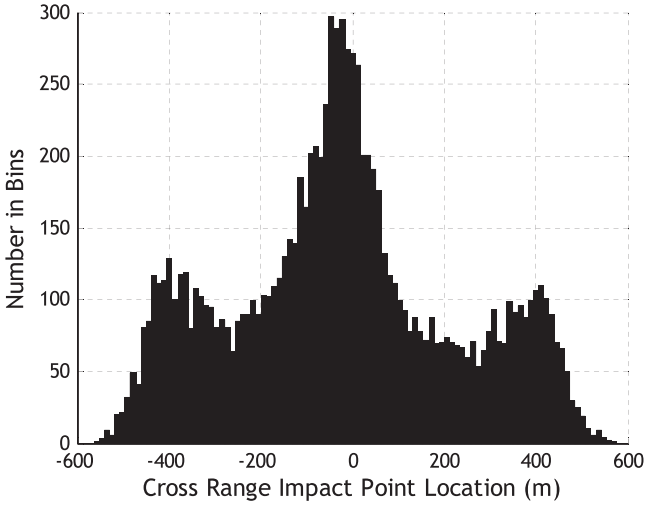

Figure 11. Histogram of cross-range impact location, 3.0 MW turbine, 40% fragment.

against blade fragment impact since there is a significant chance that a thrown blade fragment could impact beyond the setback distance. Even in the case when a setback might provide adequate protection for a specific turbine, the same setback applied to a different turbine could potentially provide no protection at all. Therefore, it would be useful to develop a methodology for determining setbacks that could provide uniform protection for various turbine sizes.

3.3. Normalization by blade fragment mass center velocity

Overlaying percentage-distance traces from Figures 12–14 for each turbine demonstrate how blade fragment throw distance varies for turbines of different size. Figure 15 shows the percentage of blade fragment ground impacts contained within circles of varying radii for 20 and 100% blade throw for each turbine. Note that although the curves have similar shape, they spread out considerably for distances greater than that corresponding to 50% of impacts contained. Furthermore, despite conventional rules of thumb stipulating that maximum throw distance increases with turbine size, Figure 15 demonstrates that the 1.5 MW turbine displays a maximum throw distance of approximately 200 m farther than the 3.0 MW turbine for 20% fragments, even though the 3.0 MW turbine has a larger blade radius and identical rotor hub height.

The fact that the largest throw distance occurs for the 1.5 MW turbine is explained by noting that this turbine has the largest tip velocity of the three examples considered. As described in Section 2.3, blade fragment release velocity is the

Wind Energ. 2012; **15**:289–303 © 2011 John Wiley & Sons, Ltd.
DOI: 10.1002/we

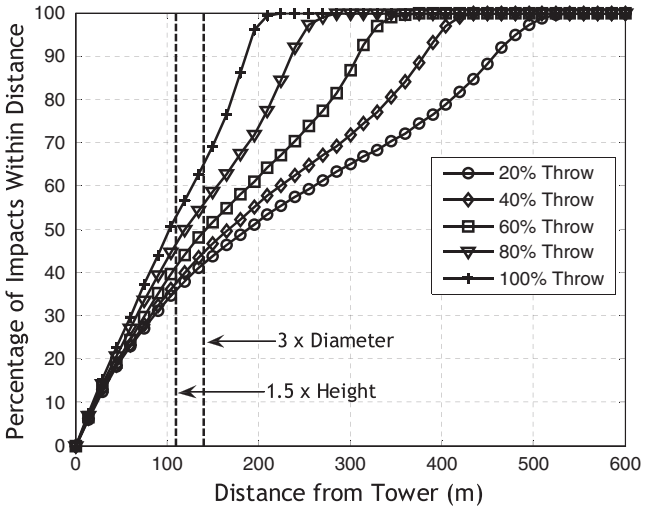

Figure 12. Percentage of impacts within distance versus distance from tower, 0.66 MW turbine.

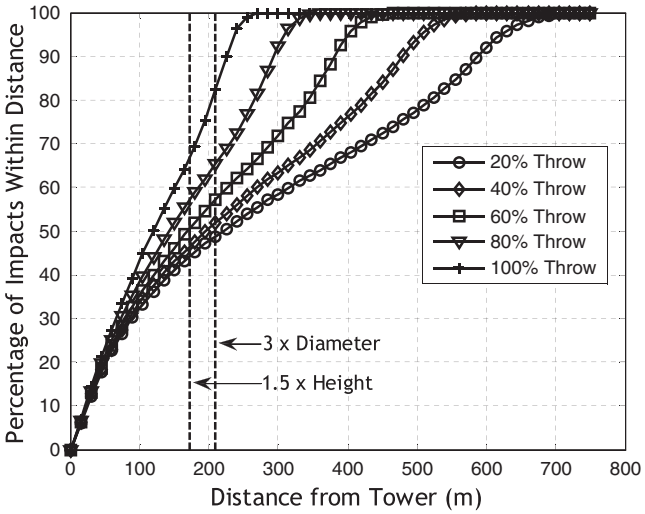

Figure 13. Percentage of impacts within distance versus distance from tower, 1.5 MW turbine.

driving factor in the determination of the maximum lateral throw distance. To verify this, the expression in equation (15) was used to numerically determine the maximum theoretical lateral throw distance of each example turbine for a 20% blade fragment. The results are shown in Table III. The lateral throw distances in Table III are somewhat less than the maximum throw distances determined through Monte Carlo simulation, since the equation does not include the effect of fragments being carried by the wind, which causes significant longitudinal displacement of impacts. However, the estimates in Table III verify that the 1.5 MW turbine should achieve the largest throw distance overall, assuming that blade fragments from all turbines are equally affected by wind after release.

Normalizing throw distance by the velocity of the blade fragment mass center for each fragment size accounts for variations in tip speed for different turbine models. This normalization procedure causes all percentage-distance traces to move significantly closer to one another regardless of fragment size. Figure 16 shows percentage-distance traces normalized by fragment mass center velocity for 20 and 100% blade fragments. Unlike Figure 15, traces are much more uniform, especially for larger fragment sizes which are less affected by winds. Figure 17 generalizes this result to all fragment sizes, showing 15 different percentage-distance traces corresponding to the five different blade fragment sizes varying from 20 to 100% for the three turbines considered. For the most part, the traces are similar and close together. However, as fragment size decreases, wind effects become more pronounced, and fragments are carried farther. This accounts for the slight spreading of the curves near maximum range.

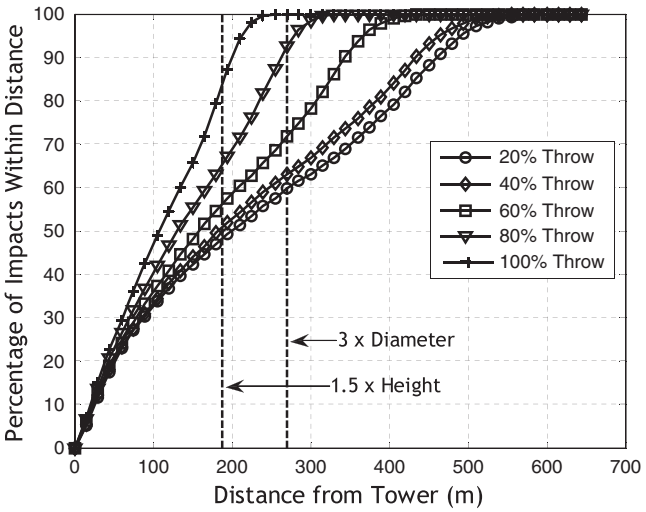

Figure 14. Percentage of impacts within distance versus distance from tower, 3.0 MW turbine.

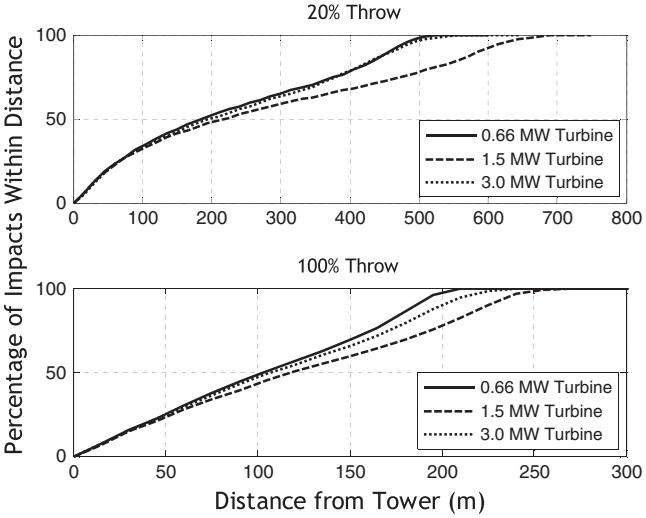

Figure 15. Percentage of impacts within distance versus distance from tower for each turbine.

Table III. Example turbine tip speed and theoretical maximum lateral throw distance of 20% fragment.

Turbine (MW)	Tip speed (rad s^{-1})	Theoretical maximum throw distribution (m)
0.66	70.03	439
1.5	80.50	590
3.0	76.05	526

3.4. Risk-based setback standard development

The normalized percentage-distance curves shown in Figure 17 form the basis for the development of a new turbine setback standard. The relationship shown in Figure 17 can be accurately approximated using a best-fit line. This best-fit line, shown in Figure 18, is given by

$$\text{Percentage of impacts inside distance} = 11.9\,\text{s}^{-1} \times \frac{\text{Distance from tower (m)}}{\text{Fragment CG release velocity (m s}^{-1})} \tag{16}$$

Wind Energ. 2012; **15**:289–303 © 2011 John Wiley & Sons, Ltd.
DOI: 10.1002/we

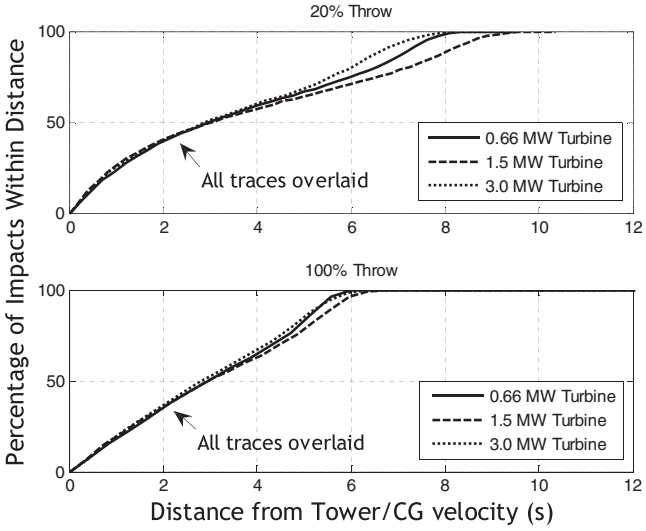

Figure 16. Percentage of impacts within distance versus normalized distance for each turbine.

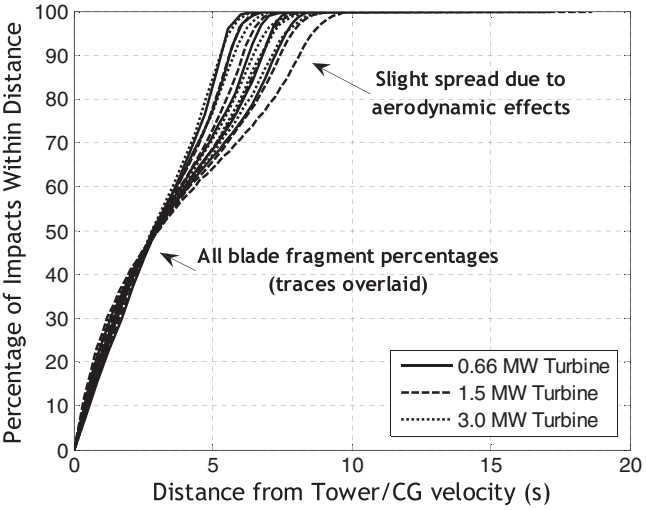

Figure 17. Percentage of impacts within distance versus normalized distance for each turbine, all fragment sizes.

It is clear based on the relationship shown in equation (16) that 99.9% of blade fragment impacts falls within a circle of radius 8.4 times the fragment CG release velocity in meters per second, where the multiplier 8.4 has the unit of seconds. Note that this can be easily computed for a specific turbine and a fragment of a given size.

Equation (16) is a powerful tool that can be used to compute appropriate setback distances for a wide variety of turbine platforms. However, this expression must be used in conjunction with several other parameters in order to produce a meaningful setback. These parameters are the probability that the turbine throws a blade or blade fragment over a given period of time, the minimum size blade fragment of concern, and the desired probability of impact greater than or equal to a certain distance if a blade throw does occur.

The following is an example case demonstrating how equation (16) can be used to determine a risk-based setback. Suppose a regulator or wind farm developer wishes to determine the proper setback distance for a single Vestas 2.0 MW turbine (Vestas Wind Systems A/S, Randers, Denmark) such that in a single year, the probability that a blade fragment will be thrown a distance equal to or beyond the setback is 5.0×10^{-5} (or one occurrence per year for every 20,000 turbines). Further, suppose that the regulator or developer is concerned only with the impact of fragments greater than or equal to 2 m in length. Table IV describes specifications of the Vestas 2.0 MW turbine under consideration here. First, by using the specifications outlined in Table IV, the 2 m blade fragment mass center release velocity is found to be 68.3 m s^{-1},

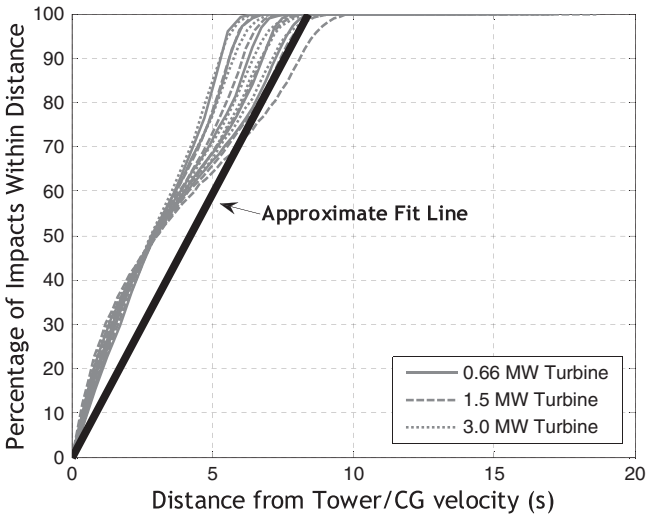

Figure 18. Linear fit to percentage versus distance data.

Table IV. Specifications for Vestas 2.0 MW turbine.

Rotor radius (m)	40
Tower height (m)	67
Rotor rotational speed (rad s^{-1})	1.75

assuming the fragment mass center is located in the middle of the fragment. Second, the probability that given a blade fragment release, the fragment lands outside the setback distance must be computed. This is accomplished by dividing the desired yearly probability that a fragment will fly to or beyond the setback by the probability that a blade failure will occur in a given year. A commonly accepted probability of blade failure per turbine per year, outlined in Rademakers and Braam,[10] is 2.6×10^{-4}. Therefore, the probability that given a fragment release, the fragment will land outside the setback distance must be equal to 0.1923. The percentage of impacts contained within the setback distance from the turbine base, the left-hand-side of equation (9), is given by $100\times(1-0.1923)=80.77\%$. Thus, equation (16) can be used to compute the desired setback distance of approximately 463 m. Note that this identical analysis can be universally applied to a variety of modern turbine designs, fragment sizes and accepted risk levels. Also, it should be noted that only the smallest fragment size of concern should be used in the proposed method of setback determination, since in general, the smallest fragments will fly farthest because of higher release velocities at the fragment mass center. Thus, all larger fragments will have a lower probability of impact outside the computed setback distance.

It is important to note that rotor overspeed situations can lead in some cases to blade throw and are not taken into account in the setback development proposed here. However, after extensive study of actual wind turbine blade failures over the course of many years, Rademakers and Braam[10] place the probability of blade failure because of an overspeed situation at 5.0×10^{-6} per turbine per year. This probability is far less than the overall blade fragment release probability of 2.6×10^{-4}, since such incidents would require the failure of multiple safety mechanisms that are becoming increasingly reliable, and thus, rotor overspeed scenarios are not included in the analysis conducted here.

4. CONCLUSION

Wind turbine setback standards designed to protect people, property and infrastructure from impact by thrown blade fragments play an important role in wind farm planning and can often be a determining factor in the number of turbines that can be placed within a given parcel of land. Given the critical importance of these regulations, there is a desire to develop setback standards based on a physical model of blade throw rather than arbitrary rules of thumb. First, a physical model for full or partial blade throw based on rigid body dynamics was described. This model, coupled with Monte Carlo simulation techniques, was used to simulate tens of thousands of blade throws for three example wind turbines of varying size. It was shown that typical current setback standards do not provide adequate protection in most cases. Then, the importance of fragment release velocity in determining maximum throw distance was analytically demonstrated, and its effect verified through analysis of Monte Carlo results. Normalizing throw distance by fragment release velocity yielded a near-linear

Wind Energ. 2012; **15**:289–303 © 2011 John Wiley & Sons, Ltd.
DOI: 10.1002/we

relationship between this normalized distance and the percentage of impacts that lie within this distance from the turbine. A final example used this relationship to determine a proper setback distance for an example turbine based on an acceptable level of risk. Setback development using this methodology allows regulators to mitigate risk using valid engineering analysis rather than arbitrary rules that provide inconsistent and inadequate protection.

REFERENCES

1. Eggwertz S, Carlsson I, Gustafsson A, Linde M, Lundemo C, Montgomerie B, Thor S. Safety of wind energy conversion systems with horizontal axis. *Technical Note HU-2229*, Flygtekniska Försöksanstalten (FFA—The Aeronautical Research Institute of Sweden), Stockholm, 1981.
2. Macqueen JF, Ainsilie JF, Milborrow DJ, Turner DM, Swift-Hook DT. Risks associated with wind turbine blade failures. *IEE Proceedings, Part A—Physical Science, Measurement and Instrumentation, Management and Education* 1983; **130**: 574–586.
3. Turner D. A Monte Carlo method for determining the risk presented by wind turbine blade failures. *Wind Engineering* 1986; **11**: 1–20.
4. Eggers AJ, Holley WE, Digumarthi R, Chaney K. Exploratory study of HAWT blade throw risk to nearby people and property. *Proceedings of the 2001 ASME Wind Energy Symposium*, Reno, Nevada, 2001; 355–367.
5. Montgomerie B. Horizontal axis wind turbine blade failure, blade fragment six degrees of freedom trajectory, site risk level prediction. *Fourth International Symposium on Wind Energy Systems*, Stockholm, Sweden, HRA Fluid Engineering, 1982; 389–401.
6. Sørensen J. On the calculation of trajectories for blades detached from horizontal axis wind turbines. *Wind Engineering* 1984; **8**: 160–175.
7. Sørensen J. Prediction of site risk levels associated with failures of wind turbine blades. In *European Wind Energy Conference*. H.S. Stephens & Associates: Bedford, England, 1984; 344–349.
8. Turner D. An analysis of blade throw from wind turbines. In *Wind Energy and the Environment*, Swift-Hook PDT (ed.). Peter Peregrinus Ltd: London, 1989; 112–135.
9. Slegers N, Rogers J, Costello M, Puga M, Arons P. Modeling the risk of a failed wind turbine blade impacting a power transmission line. *Wind Engineering* 2009; **33**: 587–606.
10. Rademakers L, Braam H. Analysis of risk-involved incidents of wind turbines. In *Guide for Risk-Based Zoning of Wind Turbines*. Energy Research Centre of the Netherlands, 2005.
11. Larwood S, Van Dam CP. Permitting setback requirements for wind turbines in California. *CEC-500-2005-184*, California Energy Commission, PIER Renewable Energy Technologies, 2006.
12. Southern California Edison. *Interconnection Handbook*. Transmission and Interconnection Planning Department, 2009; 30.
13. Daniels K. Wind Energy Model Ordinance Options. New York Planning Commission, 2005; 9.